Landslide Monitoring and Potential Assessment from Differential Interferometric Radar Analysis and Ground Instrumentations

Kuo-Lung WANG[1*], Jun-Ting LIN[1], Yi-Hsuan LEE[1], Li-Wen CHEN[1], Jheng-Ru LAI[1], Tsung-Wen CHEN[1], Yo-Ming HSIEH[2], Meei-Ling LIN[3], Ray-Tang LIAO[4], Chao-Wei CHEN[4] and Ching-Weei LIN[5]

[1] Dept. of Civil Engineering, National Chi Nan University (Puli, Nantou, Taiwan)
[2] Dept. of Construction Engineering, National Taiwan University of Science and Technology (Taipei, Taiwan)
[3] Dept. of Civil Engineering, National Taiwan University (Taipei, Taiwan)
[4] Safe Consultant Co. (Taipei, Taiwan)
[5] Dept. of Earth Sciences, National Cheng Kung University (Taipei, Taiwan)
*Corresponding author. E-mail: klwang@ncnu.edu.tw

Typhoons and earthquakes attack Taiwan every year even by month. Landslide hazard mitigation is very important in hazard prevention chain. Synthetic aperture radar images acquired by JAXA (Japan) are used in this research to monitor landslide displacement in large area. The study is trying to propose a method to produce landslide potential map from differential interferometric synthetic aperture radar (DInSAR). Small baseline subset (SBAS) is adopted for higher accuracy. This method searches points with the same radar signal strength through observing years and keep tracking locations in each scene. The RMS error directly from radar shows 10mm with 95% confidence. MEMs accelerometer with tilt and dynamic signal are also collected for ground motions. However, locale tilt or acceleration cannot reflect overall deformation. Thus a single/dual frequency GPS system is also installed in study area. The result of one monitoring landslide during a heavy rainfall event in June, 2017. The results also proved that SBAS method derived displacement map.

Key words: Landslide, SAR, MEMS, GPS

1. INTRODUCTION

Taiwan locates in the collision zone of sea plate and continental plate, which inducing earthquake and orogeny. Moreover, this island is surrounded with warm and cool sea water. Typhoons and heavy rainfall attacked this island frequently, especially after year 2000. Several typhoons and heavy rainfall with unexpected large rainfall attacked Taiwan in past 10 years. Typhoon Morakot in 2009 brings maximum 3,000 mm accumulated rainfall and the rainfall is 3/4 of average annual precipitation.

Landslide potential map is the first work for landslide hazard mitigation. There are several methods to produce landslide potential map. The logistic regression method combines potential factors with landslides and give landslide potential prediction. Two major categories including bivariate analysis and multivariate analysis are used in logistic regression analysis. Gupta and Joshi (1990) used Landslide Nominal Risk Factor (LNRF) to derive dimensionless factors and calculate the potential risk. Jade and Sarkar (1993) adopted Information Theory and classified the potential risk into three classes. Keefer (2000) proposed a landslide concentration (LC) factor to establish the relationship between landslide and earthquake. The landslide susceptibility mapping using bivariate analysis without seismic condition was conducted by different researchers. [Çevik et al., 2003; Chau et al., 2004; Lee, 2004; Lee et al., 2004; Lee, 2005; Ohlmacher and Davis, 2003]. However, the bivariate analysis does not take into account the independency of factors. Therefore, multivariate analysis has been developed for that purpose. The independency of factors must be checked and the matrix of factors is thus established.

Two classification algorithms – logistic regression and discriminating analysis are the most well-known methods to identify the susceptibility of landslide. Lin and Tung (2004) used structural equation model to establish a measuring matrix for landslide evaluation for the cases of Chi-Chi earthquake. Süzen and Doyuran (2004) compared the landslide susceptibilities using bivariate and multivariate analysis (logistic regression) based on northwest Turkey study area.

The neural network analysis uses factors related to landslides to perform training and evaluation of landslide susceptibility. The accuracy can be as high as 90% in the same area and using same event (Lee et al., 2003). However, the training process needs to restart when encountering different condition.

Semi-logistic regression methods which combined factor of safety to produce probability of landslide can be used to establish the susceptibility map. Pack et al. (1998, 1998a, 2001) used the stability index derived from factor of safety to classify susceptibility into several groups: stable, moderately stable, quasi-stable, lower threshold, upper threshold, and defended. Lan et al. (2004) used the module to analyze the landslide hazard in Yunnan, China. Another semi-logistic method adopts displacement as the index of landslide susceptibility. Wang et al. (2010) proposed a semi-mechanical and semi-regression method to produce landslide potential map.

The study is trying to propose a method to produce landslide potential map from differential interferometric synthetic aperture radar (DInSAR). Potential landslide zones are mapped after fringes and displacements are generated from ALOS/PALSAR radar image processing. Meanwhile, a deep-seated landslide site has been selected for instrumentation. Monitoring data more than 5 years has been collected and analyzed to find relationship between landslide displacement and rainfall, and groundwater. Mems accelerometer is designed for active or quick displacement area. The design is considered tilt and dynamic data collection.

2. METHODOLODY

2.1 Study area and geological condition

The study area is located at central Taiwan and the elevation ranges from 1000m to 2500m. A landslide potential map was mapped by expert from LiDAR data, which means the scars were generated by some events with unknown years and unknown active status. Most aspects of scars are facing north or south-north owing to geological condition. The geological condition in this area is quite unique, which is slate of Lushan Formation, Miocene. Lushan Formation is slate interlayered with thin metamorphosed sandstone and slate. The dip angles of slate in this area ranges from 20-70 degrees owing to gravity and tectonic forces.

2.2 Leveling verification

In order to discover landslide displacement without monitoring data, leveling data from government is a better solution to discover. However, Chi-Chi earthquake attacked Taiwan in 1999 and resulted large displacement in central Taiwan. Previous leveling data is too difficult to compare with recent result. There are only two leveling data, which are 2002 and 2009, can be found from government. Leveling was executed from Taiwan's originated point – Hutzushan to the mountain area with 1mm±1ppm accuracy. The differences between 2002 to 2009 in elevation is as shown in **Fig. 1** The differences are almost increasing except some benchmarks. The increasing of elevation is undoubtedly the effect orogeny. If rank the elevation difference and select a threshold for stable zone, the others can be eliminated the average value of stable zone. Thus benchmark C032, C034, C035 and C036 located at the river side and assumed as the elevation change to zero. The other benchmark elevations are modified from that. The benchmarks locate in landslide scars can be identified and the true landslide displacement can be calculated based on this assumption as shown in **Fig. 2**. There are four benchmarks show elevation decreasing, which means locate in landslide scars and moving between 2002~2009. The displacement has been calculated as shown in **Table 1**. The values have been transferred to annual velocity for DInSAR comparison.

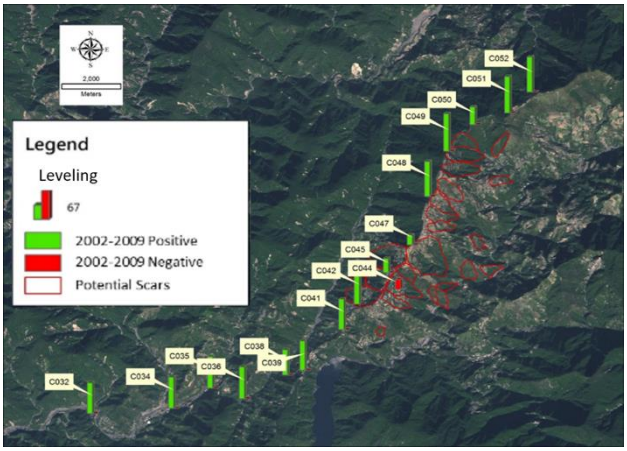

Fig. 1 The elevation change from benchmark survey in 8 years (2002-2009)

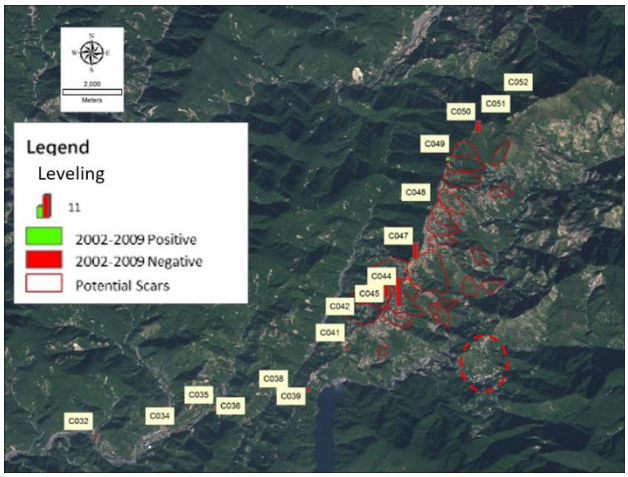

Fig. 2 Elevation differences adjusted for landslide displacement

Table 1 Elevation differences derived for landslide velocity

Benchmark Number	Relative decreasing velocity (mm/year)
C050	8.02
C047	12.03
C045	9.90
C044	22.06

2.3 Past monitoring condition

Soil and Water Conservation Bureau initiated a monitoring project in study area from 2005 to 2006. Central Geological Survey followed the monitoring system and started a long-term monitoring project from 2007. We collected data from these projects and carefully check abnormal conditions. **Fig. 3** illustrates how the monitoring works were aligned in the slope locations. The slope located in the circle area of **Fig. 2**. The prefix E denotes in-hole extensometer, A denotes ground water observation well with slope indicator, and SAA denotes shape acceleration array. Relationship between rainfall and groundwater is as shown **Fig. 4**. The figure shows that groundwater is highly related to rainfall but varies with their location within the slope. Also **Fig. 5** shows rainfall condition with groundwater level variance at site A-20. The result shows that regression has better result once lower rainfall events were removed from database. The same condition also revealed in **Fig. 6**, which is Shape Acceleration Array (SAA) displacement monitoring results comparing with accumulated rainfall events.

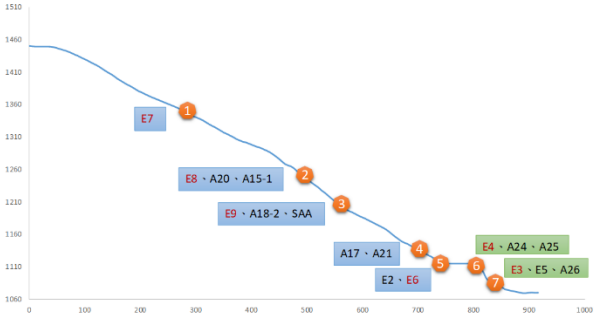

Fig. 3 The location of monitoring system on slope

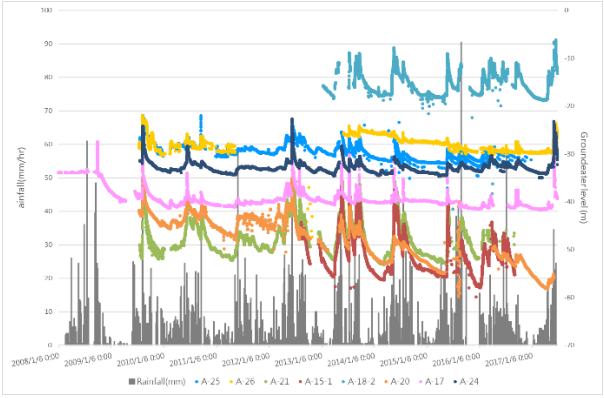

Fig. 4 The relationship of rainfall versus groundwater level

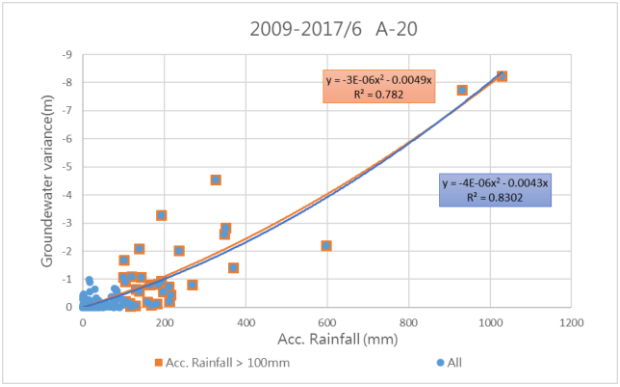

Fig. 5 Typical rainfall versus groundwater variance

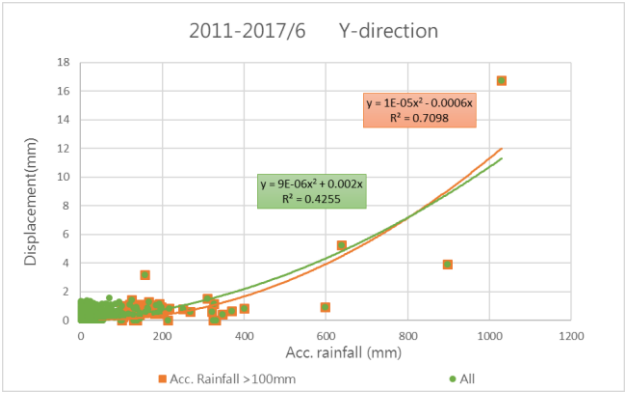

Fig. 6 Demonstration of displacement versus rainfall in study area

2.4 Potential landslide mapping with DInSAR

SAR measures the distance between satellite and ground surface by sending and receiving radar signals. Measurement of ground topography using SAR represents two locations of antenna that sensing the surface and are separated by a baseline. If the viewing geometry is controllable or known with sufficient accuracy, then the topography can be derived from the phase measurement of the two sensing radar waves. The topography can be obtained by geometry of satellite and observation point. Two important conditions that need to be understood for detecting and measuring surface change with SAR are:

(1) The changes between two successive images must not be too large.

(2) The radar-scattering characteristics within each pixel must remain similar.

The deformation of ground surface derived from DInSAR could be less than centimeter with high accuracy digital elevation model. When doing interferometry analysis by temporal SAR data, the phase information generated is including topography, change of ground characteristics, ground movement and atmosphere effect, etc. Phase difference of topography can be removed by high accuracy digital elevation model and short base line. Atmosphere effect can be reduced by long term analysis. The deformation can be trusted to high precision and after removed previous described errors and simply left ground deformation and noise.

DInSAR, PS, and SBAS has been well developed in recent years thus the monitoring of landslide displacement is becoming more possible. [Pieraccini et al. 2003, Tarchi et al. 2003, Guzzetti et al. 2009, Cal al. 2013, Liu et al. 2013, Lowry et al. 2013, Jebur et al. 2015, Tang et al. 2015, Casagli et al. 2016, Uhlemann et al. 2016].

The SAR images used in this research is Advanced Land Observing Satellite (ALOS) Phased Array type L-band Synthetic Aperture Radar (PALSAR) and ALOS-2 L band image. The polarization of radar electromagnetic wave is Horizontal - Horizontal (HH) mode and incident angle is 34.3 degree. The range resolution from this area is approximately 10 meter. There are several SAR images can be used for differential interferometric SAR. However, ALOS PALSAR/ALOS2 with L band has longer wave length, which is 23cm and possible could be eliminated the effect of vegetation.

DInSAR method is fine to observe landslide scar at two images with close dates. However, the displacement data shows too much noise to identify accuracy and comparison with benchmark data. An example of DInSAR event is as shown in **Fig. 7**, the even is typhoon Morakot with about 1000mm rainfall in study area. The result shows some displacement signal within landslide but not obvious.

Thus another approach small baseline subset (SBAS) is adopted for higher accuracy. This method searches points with the same radar signal strength through observing years and keep tracking locations in each scene. SBAS analysis is performed with only 13 ALOS images owing to lack of small baseline dataset. The RMS vertical displacement error directly from radar shows 10mm with 95% confidence. The ALOS satellite was not in function after 2011 until ALOS2 was back to track in 2014. The ALOS data with previous analysis combining with 6 ALOS2 images are adopted for analysis in study area. SBAS analysis result combining ALOS with ALOS2 is as shown in **Fig. 7**. The RMS vertical displacement error directly from radar shows 7.6mm with 95% confidence. The result combing ALOS/ALOS2 images not only reveals more displacement data points but also show more fit with mapped scars previous described. Two fastest landslide masses are found in study area within landslide scars as shown in **Fig. 8.** GPS monitoring were initiated to verify SBAS analysis result.

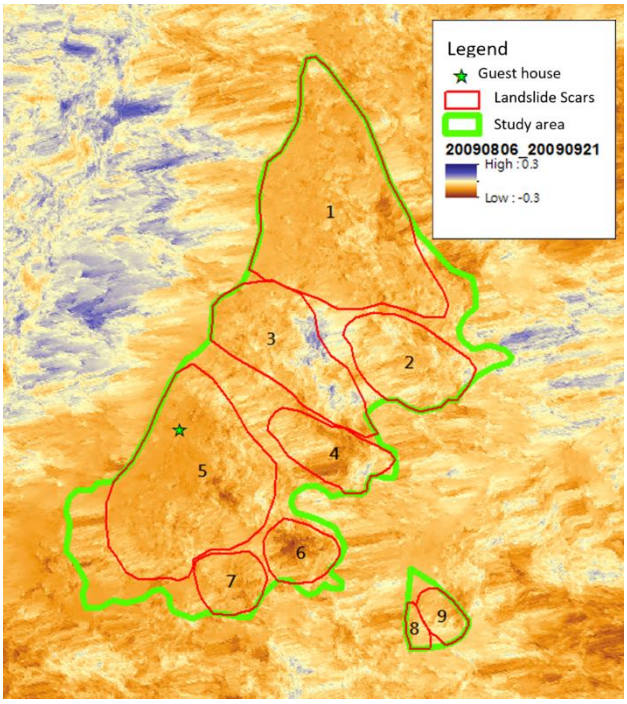

Fig. 7 Displacement map derived from DInSAR between tyhoon Morakot event in 2009 (unit: m)

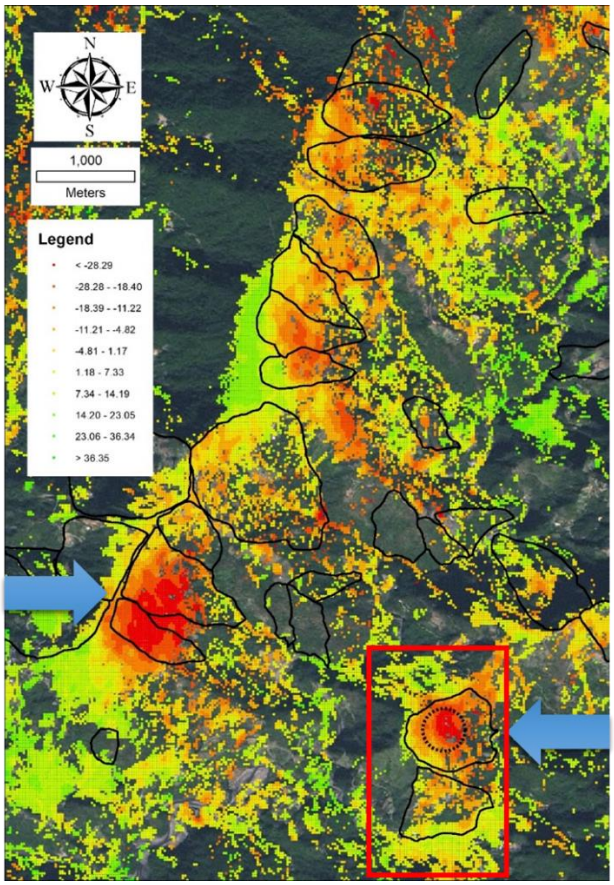

Fig. 8 Vertical displacement velocity map produced with SBAS (2007-2017/07) (unit: mm/year)

2.5 Low-cost mems accelerometer monitoring

Owing to landslide instrumentation is too expensive and unnecessary. In this work, we present a low-cost slope-monitoring device. The device is constructed using components purchased online at reasonable costs. The device is capable of recording triaxial accelerations at 200Hz onto standard SD (secure digital) memory cards. In addition, the sensed triaxial accelerations can be converted to tilt, which can then be sent via onboard GPRS module to a cloud server. Thus, the constructed device can be used for both static measurements of the slope surface and dynamic measurements of ground-surface acceleration. This information can assist assess slope condition regularly and dynamic force experienced by the slope after earthquake. **Fig. 9** illustrates distribution of dual frequency GPS and MEMs installed in to selected landsides, which are as shown rectangular in **Fig. 8**. The recorded data has been calculated to tilt as shown in **Fig. 10**. The results shows the tilt direction s toward landside direction at toe.

Fig. 9 Locations of dual frequency GPS and MEMs

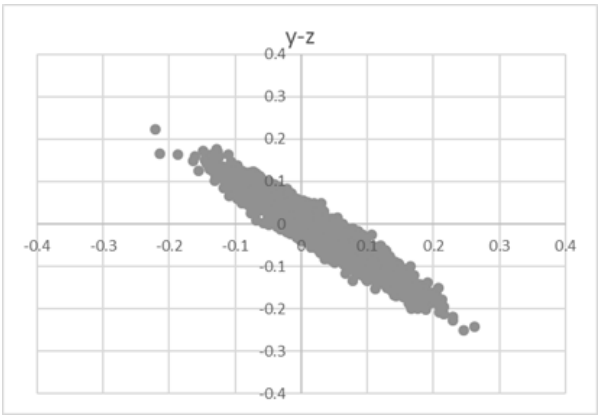

Fig. 10 Tilt derived from MEMS accelerometer of Y-Z plane

2.6 GPS monitoring

GPS monitoring system were initiated for monitoring landslide activity after DInSAR results show that the study are is highly active. Five dual frequency GPS stations were set up for monitoring and verification of DInSAR result. Owing to lack f funding, GPS stations were set up in April, 2017 without funng. Two GPS solution methods are adopted in this study, which are node to node and network calculation. Open source code RTKLib was adopted as node to node solution and network solution uses commercial software MAGNET from TOPCON for comparison. **Fig. 11** shows the result at the same location of MEMS station, which shows obvious displacement and tilt direction in June, 2017 event.

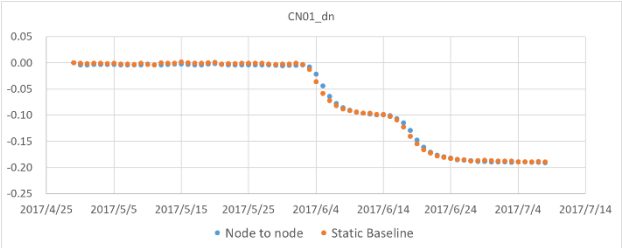

(a) Displacement of north direction

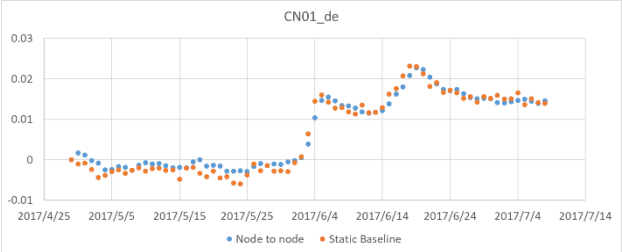

(b) Displacement of east direction

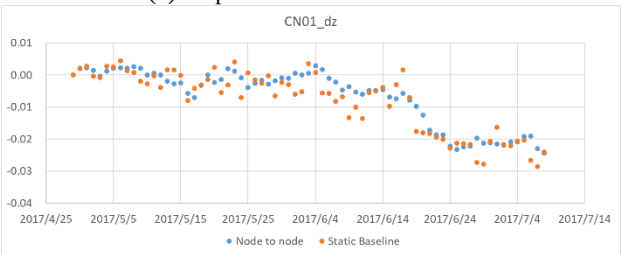

(C) Displacement of vertical direction

Fig. 11 GPS1 monitoring results at MEMS location

The other special GPS monitoring result locates at the dashed circle in **Fig. 8**. The GPS solution is as shown in **Fig. 12**. The results show -3 cm in north, 12 cm in east and -6 cm in June, 2017 rainfall event.

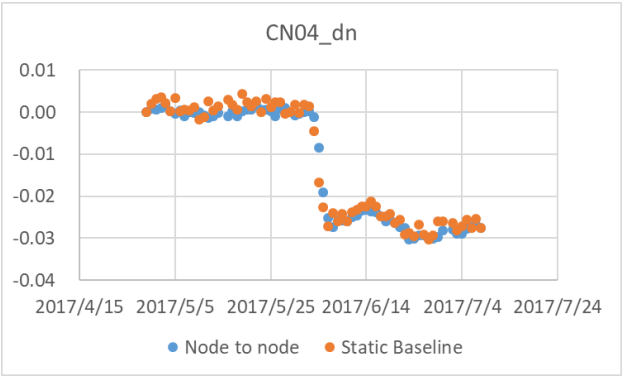

(a) Displacement of north direction

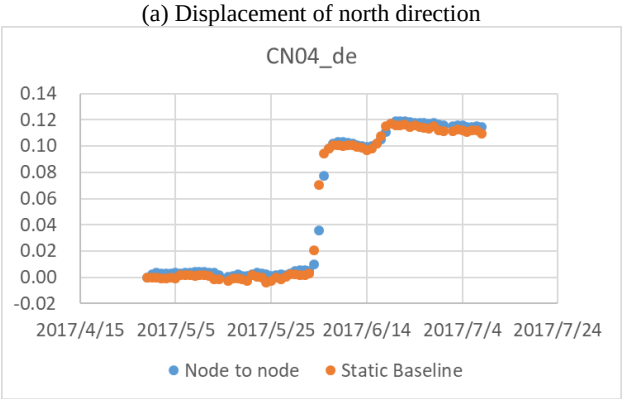

(b) Displacement of east direction

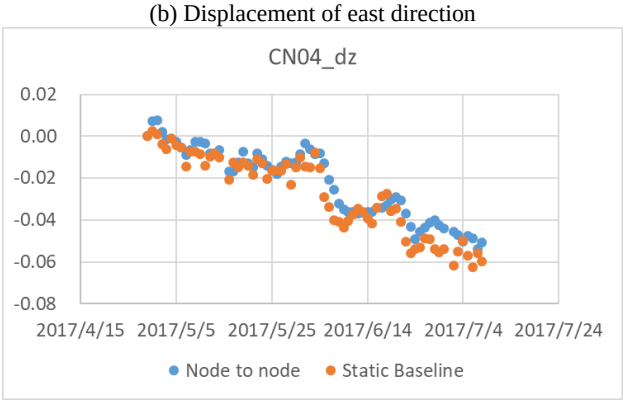

(C) Displacement of vertical direction

Fig. 12 GPS4 monitoring results at MEMS location

3. DISCUSSION

As previous described about leveling data in 8 years (2002-2009). Benchmark number C044 shows 22mm/year gradually sliding down. The SBAS analysis result at the same point from 2007 to 2017 is as shown in **Fig. 13**. According to benchmark survey data, the elevation lowering velocity is about 22mm/year, which means approximately 220mm from 2007 to 2017. The results shows a slightly difference from SBAS result in **Fig. 13** but still have the same trend. Also the elevation has a significant difference during heavy rainfall event in 2017.

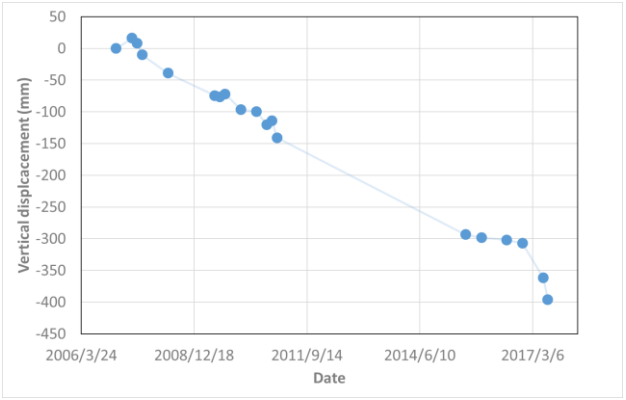

Fig. 13 Vertical displacement of benchmark number C044 point from SBAS

In order to verify the accuracy of SBAS analysis result, a dual frequency GPS was installed for analysis at the center of dashed line circle in **Fig. 8**. Vertical displacement at the same point of SBAS analysis result was extracted and as shown in **Fig. 14**. The figure shows vertical displacement is continuously sliding down and has a jump in 2017 owing to a heavy rainfall event in June. The event resulted in 1500mm rainfall in two weeks. According to SBAS result from Dec., 2016 to July, 2017, vertical displacement calculated is about 8cm at this

point. A dual frequency GPS was installed in April, 2017 to verify SBAS result. A refer GPS station located at stable location 1.1km away from this point is adopted for node to node displacement calculation. Three dimensional GPS displacement of June event was calculated as shown in **Fig. 12**. The displacement toward east about 11cm, south about 3cm and down about 6cm from April to August. The monitoring period difference is from January to April in 2017. However, the results of two differential methods reveal high accuracy result. However, SBAS results are not easy to compare with GPS data owing to GPS monitoring initiated from 2017. The only way to verify long term landslide deformation is from leveling data. The displacement shows good coincidence when treat leveling data from displacement magnitude to velocity. Moreover, the GPS installed from April, 2017 monitored an event in June, 2017, which displacements measured are the same with SBAS results.

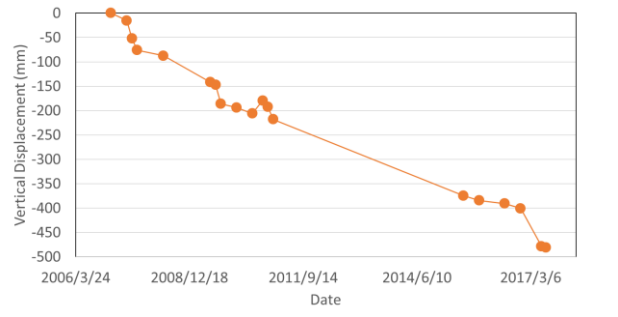

Fig 14 Vertical displacement derive from ALOS/ALOS 2 SBAS analysis

4. CONCLUSIONS

Landslide potential map is typically generated by factors by statistic method or mechanic equilibrium approach. In this work we propose a monitoring methodology from DInSAR and SBAS data processing. This method can identify active landslide scars in the same rainfall condition area, which means should pay more attention to monitoring. DInSAR can map landside scars from fringe and displacement map roughly. SBAS has more precise displacement monitoring and landslide boundary can be thus defined. Two deep seated landslides were selected for instrumentation to compare with DInSAR and SBAS method. SBAS results show more appropriate for active landslide mapping. The verification from GPS shows that SBAS can derive high accuracy result for landslide monitoring. Therefore large area landslide monitoring can be performed with such method and expensive monitoring instrumentation can be selected to install at fast displacement locations. Moreover, SBAS method can detect un-stable landslide and provide early warning for engineering treatment or monitoring works.

The underground instrumentations show that landslide displacement has good coincidence with accumulative rainfall. However, landslide instrumentation is too expensive when there are many potential scars in study area. Thus a low-cost mems monitoring sensor was developed in this work. In this work, we share our experience on building a low-cost slope-monitoring device that senses temperature and dynamic accelerations at 200Hz, provides 6-month long-term storage with a 16GB micro SD card, and sends calculated tilt to cloud servers via GPRS module. The low-cost system works well and provides more quick response to landslide warning much earlier than DInSAR and SBAS methods.

ACKNOWLEDGMENT: The authors would like to present their grateful thanks for the research grant from Ministry of Science and Technology and research possibilities from Central Geological Survey, Taiwan.

REFERENCES

Cal, F., F. Ardizzone, R. Castaldo, P. Lollino, P. Tizzani, F. Guzzetti, R. Lanari and M. Manunta (2013) Landslide analysis through the multi-sensor SBAS-DInSAR approach: The case study of Assisi, Central Italy. 2013 IEEE International Geoscience and Remote Sensing Symposium - IGARSS. 2916-2919.

Casagli, N., F. Cigna, S. Bianchini, D. Hölbling, P. Füreder, G. Righini, S. Del Conte, B. Friedl, S. Schneiderbauer, C. Iasio, J. Vlcko, V. Greif, H. Proske, K. Granica, S. Falco, S. Lozzi, O. Mora, A. Arnaud, F. Novali and M. Bianchi (2016) Landslide mapping and monitoring by using radar and optical remote sensing: Examples from the EC-FP7 project SAFER. Remote Sensing Applications: Society and Environment 4: 92-108.

Chau, K.T., Y.L. Sze, M.K. Fung, W.Y. Wong, E.L. Fong and L.C.P. Chan (2004) Landslide hazard analysis for Hong Kong using landslide inventory and GIS. Computers and Geosciences. 30:429-443.

Gupta, R.P and B.C. Joshi (1990) Landslide Hazard Zoning Using the GIS Approach – A Case Study from the Ramganga Catchment, Himalayas. Engineering Geology. 28:119-131.

Guzzetti, F., M. Manunta, F. Ardizzone, A. Pepe, M. Cardinali, G. Zeni, P. Reichenbach and R. Lanari (2009). Analysis of Ground Deformation Detected Using the SBAS-DInSAR Technique in Umbria, Central Italy. Pure and Applied Geophysics. 166(8): 1425-1459.

Jade S. and S. Sarkar (1993) Statistical models for slope instability classification. Engineering Geology., 36:91-98.

Jebur, M. N., B. Pradhan and M. S. Tehrany (2015) Using ALOS

PALSAR derived high-resolution DInSAR to detect slow-moving landslides in tropical forest: Cameron Highlands, Malaysia. Geomatics, Natural Hazards and Risk 6(8): 741-759.

Keefer D.K. (2000) Statistical analysis of an earthquake-induced landslide distribution – the 1989 Loma Prieta, California event. Engineering Geology. 58:231-249.

Lan H.X., C.H. Zhou, L.J. Wang, H.Y. Zhang and R.H. Li (2004) Landslide hazard spatial analysis and prediction using GIS in the Xiaojiang watershed, Yunan, China. Engineering Geology. 76:109-128.

Lee, C. N. (2001) Preliminary study on the Tsao-Ling landslide area under earthquake. Master's Thesis. National Taiwan University.

Lee S. (2004) Application of likelihood ratio and logistic regression models to landslide susceptibility mapping using GIS. Environmental Management. 34(2):223-232.

Lee S. (2005) Application of logistic regression model and its validation for landslide susceptibility mapping using GIS and remote sensing data. International Journal of Remote Sensing. 26(7):1477-1491.

Lin, M. L. and C.C. Tung (2004), A GIS-based potential analysis of the landslides induced by the Chi-Chi earthquake. Engineering Geology. 71:63-77.

Liu, G., R. Wang, Y. K. Deng, R. Chen, Y. Shao, W. Xu and D. Xiao (2013). Monitoring of ground deformation in Beijing using SBAS-DInSAR technique. 2013 Asia-Pacific Conference on Synthetic Aperture Radar (APSAR). 300-303.

Lowry, B., F. Gomez, W. Zhou, M. A. Mooney, B. Held and J. Grasmick (2013) High resolution displacement monitoring of a slow velocity landslide using ground based radar interferometry. Engineering Geology. 166: 160-169.

Ohlmacher G. C. and J.C. Davis (2003) Using multiple logistic regression and GIS technology to predict landslide hazard in northeast Kansas, USA. Engineering Geology. 69:331-343.

Pack, R. T., D.G. Tarboton and C. N. Goodwin (1998) The SINMAP approach to terrain stability mapping. The 8th Congress of the International Association of Engineering Geology, Vancouver, Canada.

Pack, R. T., D.G. Tarboton and C.N. Goodwin (1998a) Terrain stability mapping with SINMAP, technical description and user guide for version 1.00. Report Number 4114-0, Terratech Consulting Ltd., Salmon Arm, B.C., Canada.

Pack, R. T., D.G. Tarboton and C.N. Goodwin (2001) Assessing terrain stability in a GIS using SINMAP. The 15th annual GIS conference, Vancouver, Canada.

Pieraccini, M., N. Casagli, G. Luzi, D. Tarchi, D. Mecatti, L. Noferini and C. Atzeni (2003) Landslide monitoring by ground-based radar interferometry: A field test in Valdarno (Italy). International Journal of Remote Sensing. 24(6): 1385-1391.

Süzen, M.L. and V. Doyuran (2004) A comparison of the GIS based landslide susceptibility assessment methods: multivariate versus bivariate. Environmental Geology. 45:665-679.

Tang, P., F. Chen, H. Guo, B. Tian, X. Wang and N. Ishwaran (2015) Large-Area Landslides Monitoring Using Advanced Multi-Temporal InSAR Technique over the Giant Panda Habitat, Sichuan, China. Remote Sensing. 7(7): 8925.

Tarchi, D., N. Casagli, S. Moretti, D. Leva and A. J. Sieber (2003) Monitoring landslide displacements by using ground-based synthetic aperture radar interferometry: Application to the Ruinon landslide in the Italian Alps. Journal of Geophysical Research: Solid Earth. 108(B8): n/a-n/a.

Uhlemann, S., A. Smith, J. Chambers, N. Dixon, T. Dijkstra, E. Haslam, P. Meldrum, A. Merritt, D. Gunn and J. Mackay (2016) Assessment of ground-based monitoring techniques applied to landslide investigations. Geomorphology. 253: 438-451.

Wang, K.-L. and M.-L. Lin (2010) Development of Shallow Seismic Landslide Potential Map Based on Newmark's Displacement: The Case Study of Chi-Chi Earthquake, Taiwan. Environmental Earth Sciences. 60(4), 775-785.